Astaxanthin Interacts with Selenite and Attenuates Selenite-Induced Cataractogenesis

Jiahn-Haur Liao,[†] Chien-Sheng Chen,[†] Timothy J. Maher,[‡] Chiung-Yueh Liu,[§] Mei-Hsiang Lin,[§] Tzu-Hua Wu,*[,§] and Shih-Hsiung Wu*[,†]

Institute of Biological Chemistry, Academia Sinica, Taipei 115, Taiwan, Department of Pharmaceutical Sciences, Massachusetts College of Pharmacy and Health Sciences, Boston, Massachusetts 02115, USA, and School of Pharmacy, College of Pharmacy, Taipei Medical University, Taipei 110, Taiwan

Received October 11, 2008

Selenite, the most commonly encountered toxic form of selenium, in overdose, is used to induce cataracts in rats. This study demonstrated that selenite, but not selenate, would interact with the carotenoid astaxanthin (ASTX), as determined using isothermal titration calorimetry and NMR. The maximum absorption of ASTX decreased with increasing selenite concentration, indicating that the conjugated system of ASTX was changed by selenite. Such interactions between ASTX and selenite were also supported by the attenuation of selenite-induced turbidity by ASTX (0−12.5 μM) in vitro. In vivo experiments also showed that ASTX attenuated selenite-induced cataractogenesis in rats. In summary, this is the first report of a direct interaction of ASTX with selenite. This interaction is supported by an in vitro assay and may be partially responsible for the ASTX observed in vivo protection against selenite-induced cataractogenesis.

Introduction

Selenium, which was discovered in 1818 and named after the Greek goddess of the moon, Selene, had been thought to be nothing more than a poison until its identification as a micronutrient for bacteria, mammals, and birds (*1*). Like many micronutrients, selenium is required for the maintenance of numerous cell processes and the optimal activity of various enzymes. Selenium deficiency has been linked to neurodegenerative diseases (*2*), cardiovascular diseases (*3*), and cancers (*4*) by epidemiological findings. The U.S. Recommended Dietary Allowance (RDA) for selenium has been calculated as 70 and 55 μg per day for adult men and women, respectively, after correcting for differences in body size and taking into consideration possible individual variations in requirements. Recommended intake and upper tolerable levels are 40−55 and 300 μg/day, respectively (*5*). Because selenium is also toxic at intake levels only 5−10-fold above supranutritional amounts (*6*), there is a possibility that supplement abuse, and the resulting increased body burdens of selenium, may predispose individuals toward toxicity. Therefore, excess selenium can produce selenosis in humans, affecting the liver, skin, nails, and hair. Several case reports of fatalities have implicated selenium as the cause of death in acute selenium intoxication, and selenium has even been used as a homicidal agent (*7*). A previous study indicated that cataractogenesis may be caused by either an excess or a deficiency of selenium (*8*). Recently, a study noted that people with the most opaque and colored cataracts had the most selenium in the lens (*9*). It seems quite probable that accumulation of selenium in the lens can be a risk factor for cataractogenesis.

* To whom correspondence should be addressed. (T.-H. Wu) Tel: 886-2-2736-1661 ext. 6172. Fax: 886-2-2231-1412. E-mail: thwu@tmu.edu.tw. (S.-H. Wu) Tel: 886-2-2785-5696 ext. 7101. Fax: 886-2-2653-9142. E-mail: shwu@gate.sinica.edu.tw.

[†] Academia Sinica.

[‡] Massachusetts College of Pharmacy and Health Sciences.

[§] Taipei Medical University.

The most encountered forms of selenium compounds include selenocysteine, selenomethionine, selenate (SeO_4^{2-}), and selenite (SeO_3^{2-}). The organoselenium forms, selenocysteine and selenomethionine, are the most biologically relevant and are less toxic than the inorganic forms, selenate and selenite (*10*). Selenite is the most commonly encountered toxic form, whereas selenate is considered to be relatively less toxic (*11, 12*), and both have been shown in overdose to cause cataracts in rat pups (*13*−*17*). The ability of selenite to cause cataracts was first described by Ostadalova and colleagues (*16*), and now, selenite-induced cataracts constitutes a convenient animal model for studying nuclear cataracts.

Selenite-induced cataracts are usually produced by a single subcutaneous injection of excess sodium selenite into suckling rats resulting in severe, bilateral nuclear cataracts within several days. One hypothesis regarding the beginning of the cataract development suggests that selenium could oxidize the SH groups of ion transporters in the membrane that maintains ionic homeostasis (*18*). For example, the Ca-ATPase activity of the rat lens was decreased by 50% when sodium selenite was injected (*19*), and the inhibition of this calcium pump may be the most important mechanism for the observed calcium accumulation in the lens. Another observed pathology is believed to result from abnormal lenticular calcium accumulation. The reasons leading to the altered calcium permeability are ambiguous but probably result from a shifting of the oxidative status of the lens toward the pro-oxidant state of selenite. Therefore, the disruption of calcium homeostasis in the lens could be affected by antioxidant treatments.

Antioxidants such as propolis, diclofenac, vitamin C, and quercetin have been shown to delay or prevent cataract formation (*20*). Astaxanthin (ASTX), a carotenoid with potent antioxidant properties existing naturally in various plants, algae, and marine animals, is closely related to other well-known carotenoids, such as β-carotene, zeaxanthin, and lutein, and thus shares many of the metabolic and physiological functions attributed to these carotenoids (*21*). Several studies have shown

10.1021/tx800378z CCC: $40.75
Published on Web 02/04/2009

that ASTX displays wide-ranging biological activities (*22*−*28*). It also has been recently reported to possess anti-inflammatory activities (*29*) and provide significant protection against cataract formation in Atlantic salmon (*30*). ASTX is very good at protecting membranous phosphorlipids and other lipids against peroxidation (*21*−*23*).

In fact, the bathochromic shift of the absorption by ASTX in lobster crustacyanin has intrigued scientists since the 1960s (*31, 32*). The visible absorption spectrum of free ASTX in organic solvents has been documented (*31*). The charged ASTX was then proposed to explain its strong electrostatic polarizations (*33*). Other chemical evidence, such as the stability of carotenoid polyenyl cations or the new crystal structure of unbound ASTX, has been elucidated (*34*−*37*). Our laboratory has also provided evidence for the involvement of the ASTX/calcium complex in the ability of ASTX to protect porcine lens crystallins from oxidative damage and calcium-induced protein turbidity in vitro (*38, 39*).

To further explore the biological activities linked to the chemistry of ASTX, here, we established an in vitro selenite-induced lens turbidity assay. Also, evidence for the interaction between ASTX and selenite shown by ITC, NMR, and UV spectroscopy may provide a mechanism for ASTX in preventing both in vitro and in vivo selenite-induced cataractogenesis.

Experimental Procedures

General. HPLC-grade dimethyl sulfoxide (DMSO) and methanol (MeOH) were purchased from Merck Chemical Co. (Darmstadt, Germany). ASTX, sodium selenite, and sodium selenate were purchased from Sigma-Aldrich Chemical Co. (St. Louis, MO). NMR experiments were measured on a Bruker Avance 400 NMR spectrometer (400 MHz) at 300 K. Chemical shifts of ^{1}H and ^{13}C NMR spectra were reported relative to TMS (δ_H, 0 ppm) and $CDCl_3$ [δ_C (central line of t), 77 ppm], respectively. For better resolution of the ASTX/SeO_3^{2-} complex in ^{1}H NMR spectra, the mixed $CDCl_3$/DMSO-d_6/D_2O (4:4:1, v/v/v) solvent was used for the proton and carbon nuclei NMR experiments. Heteronuclear multiple-quantum coherence and heteronuclear multiple-bond correlation spectra were taken to determine the types of carbon signals.

Isothermal Titration Calorimetry (ITC). For better solubility of sodium selenite or sodium selenate, the mixed DMSO/MeOH/H_2O (2:1:1, v/v/v) solvent was used in the ITC experiment carried out with an ITC Microcalorimeter (VP-ITC, Microcal, Inc., Northampton, MA, USA). The heat produced by the complex formation while 81 μM ASTX was mixed with 2.75 mM Na_2SeO_3 or Na_2SeO_4 at 25 °C with continuous stirring (300 rpm) was analyzed using Origin software (Edition 7.0, Microcal Inc.). The integration of the heat pulses obtained from each titration was fitted to a theoretical titration curve to obtain the enthalpy change (ΔH in cal/mol), the entropy change (ΔS in cal mol^{-1} K^{-1}), the association constant (K_{assoc} in M^{-2}), and the number of binding sites (n, per compound). The dilution effect (0.2 cal/mol) produced when 5.5 mM Na_2SeO_3 or Na_2SeO_4 was injected into the vehicle was used as the baseline.

^{77}Se-NMR Titration Studies of the ASTX/SeO_3^{2-} Complex Formation. For better solubility of sodium selenite or sodium selenate, the mixed DMSO-d_6/CD_3OD-d_4/D_2O solvent was used in the ^{77}Se-NMR experiment. ^{77}Se-NMR spectra were reported relative to external diphenyl diselenide (PhSeSePh, 460 ppm). A 0.4 mL aliquot of 20 mM Na_2SeO_3 in DMSO-d_6/CD_3OD-d_4/D_2O (2:1:1, v/v/v) was transferred to a 5 mm NMR tube, and 20 mM ASTX (0.4-mL, in DMSO-d_6/CD_3OD-d_4/D_2O = 2:1:1) was then added.

UV/Vis Titration Studies of ASTX/SeO_3^{2-} Complex Formation. A working solution of 10 μM ASTX was prepared in DMSO/H_2O (3/17, v/v), and a 1 mL aliquot was transferred to a 1 cm cuvette. The sodium selenite (5 mM) and ASTX (10 μM) were mixed as SeO_3^{2-} stock solution in the same DMSO/H_2O mixture, to prevent the dilution of ASTX during the titration. The absorbance of ASTX at various ratios of ASTX/sodium selenite (1:0−1:128) was then determined with a Hitachi U-3300 spectrophotometer (Tokyo, Japan).

In Vitro Lens Crystallin Turbidity Assays. Porcine lenses were decapsulated and homogenized in buffer containing 50 mM Tris-HCl, 0.1 M NaCl, 5 mM EDTA, 0.01% β-mercaptoethanol, and 0.02% sodium azide, pH 8.0. After centrifugation at 27000g for 30 min, the supernatant was collected, and the protein concentration was determined according to the Bradford method (BioRad Laboratories, USA). The lens crystallins (65 mg/mL) were incubated with 1 and 10 mM selenite (Na_2SeO_3) or selenate (Na_2SeO_4) under similar conditions described above, and the turbidity was measured at 450 nm with an enzyme-linked immunosorbent assay (ELISA) reader for four consecutive days. The additions of various concentrations (0, 1.25, 2.5, 7.5, and 12.5 μM) of ASTX to lens preparations aimed to investigate the influence of ASTX on lens crystallin turbidity induced by selenite. In a separate experiment, 1 day incubations of the lens crystallins (115 mg/mL) with 10 mM selenite (Na_2SeO_3) or selenate (Na_2SeO_4) in PBS (10 mM $NaHPO_4$, 2 mM KH_2PO_4, 3 mM KCl, and 0.1 M NaCl, pH 7.4) buffer at 37 °C were then photographed. SDS-polyacrylamide slab gel (5% stacking/12% resolving gel) electrophoresis (SDS-PAGE) was performed as previously report (*40*).

Selenite-Induced Cataract Animal Model. Sprague−Dawley rat pups aged 10 days were obtained from the National Science Council Animal Center (Taiwan) and housed with their mothers under standard conditions. All experiments were performed in accordance with the "The Guiding Principles in the Care and Use of Animals". The rat pups were given a normal Purina rat chow and water, ad libitum. Starting from postnatal day 12, rat pups were divided into four groups (n = 5−7) and administered orally with ASTX (0.1, 0.3, and 1.0 mg/kg in 0.1 mL of olive oil) or vehicle throughout the observation period. At postnatal day 15, all pups were given a single injection of 19 μmol/kg of sodium selenite (pH 9.0) subcutaneously, except those without any treatments (the normal rats). To minimize any bias, the transparency status of their eyes was observed daily by observers blinded to the treatment protocols. Scores of the lens status included three values: 0 (extremely clear), 1 (formation of pinpoint cataract or diffuse nuclear opacity with scattering), and 2 (mature dense opacity involving the entire lens). The transparency scores were recorded for each group, and the experiments were performed in triplicate. The average scores of cataract formation for each treatment group are expressed as the mean ± SEM and analyzed statistically by Kruskal−Wallis One-Way ANOVA on Ranks with post hoc Dunn's testing (SigmaStat 2.03). The minimum significance was set at $p < 0.05$.

Results

Binding of Selenite to ASTX. Reports indicate that selenium can bind to lipids of two unicellular marine algae (*41*). Of the lipids that contain selenium, carotenoid pigments contain the greatest concentration. It is reasonable to suggest that selenite would bind to ASTX. ITC is a versatile method to study the binding affinity between two molecules. Sodium selenite (Na_2SeO_3) was used as a titrant to titrate ASTX. The results yielded an endothermic titration curve (Figure 1A). As compared to the dilution curve of ASTX with sodium selenate (<0.2 μcal/mol per injection, Figure 1B), ASTX had a selective binding affinity with the selenite ion. From the one-site fitting function with stoichiometry n = 2, the complexation between ASTX and selenite was observed with an enthalpy-capture process, larger entropy property, and a negative Gibb's free energy (ΔH = 7.65 kcal/mol, ΔS = 42.4 cal mol^{-1} K^{-1}, and ΔG = −4.99 kcal/mol). These thermal statistics indicated that the spontaneous complexation of ASTX/SeO_3^{2-} is an entropy-driven process.

Complexation of Selenite/ASTX. Figure 2 represents the ^{77}Se-NMR and ^{1}H NMR spectra of neat ASTX and the complexation of ASTX/SeO_3^{2-}. As compared to SeO_3^{2-} (1278.97

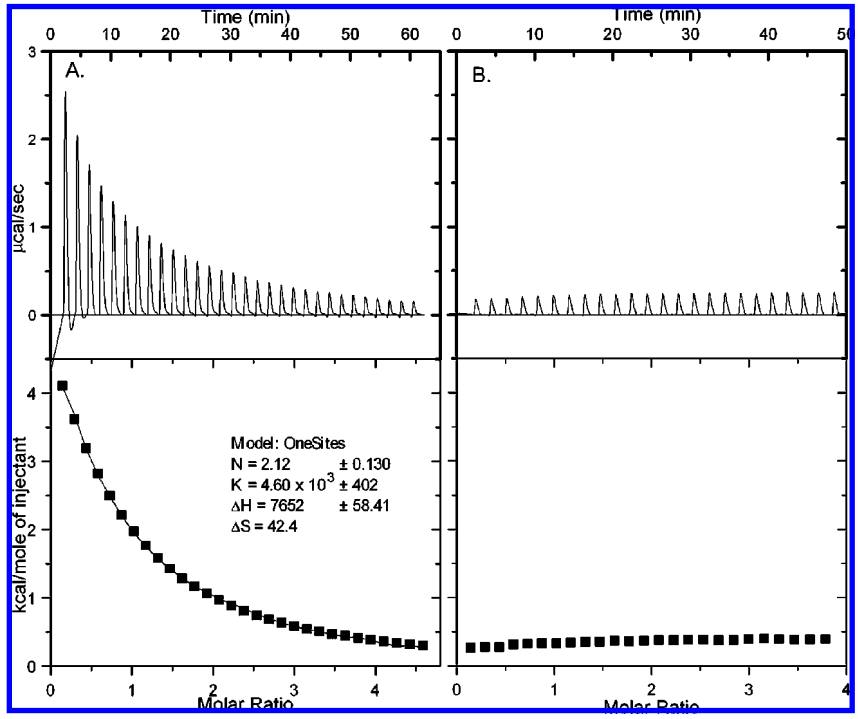

Figure 1. Interaction between ASTX and selenite was monitored by ITC. Titrations of 81 μM ASTX with 2.75 mM Na_2SeO_3 (A) and Na_2SeO_4 (B) at 25 °C were performed using a VP-ITC microcalorimeter. For the titration of ASTX/SeO_3^{2-}, raw data were obtained from 30 automatic injections (8 μL each), and the integrated fitted curves show the experimental points with the value of the parameter, $n = 2$, by using a one-site fitting function.

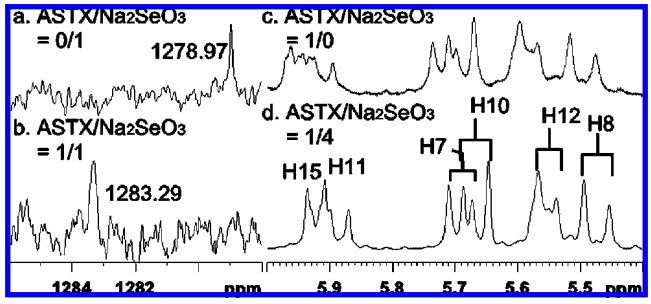

Figure 2. Interaction between ASTX and selenite was analyzed by NMR. Downfield shift in ^{77}Se-NMR spectra of Na_2SeO_3 (10 mM) alone (a) and with one equivalence of ASTX (b) in DMSO-d_6/D_2O (2:1, v/v). Upfield shift in ^{1}H NMR spectra of ASTX (2 mM) alone (c) and with four molar equivalents of Na_2SeO_3 (d) in $CDCl_3$/DMSO-d_6/D_2O (4:4:1, v/v/v).

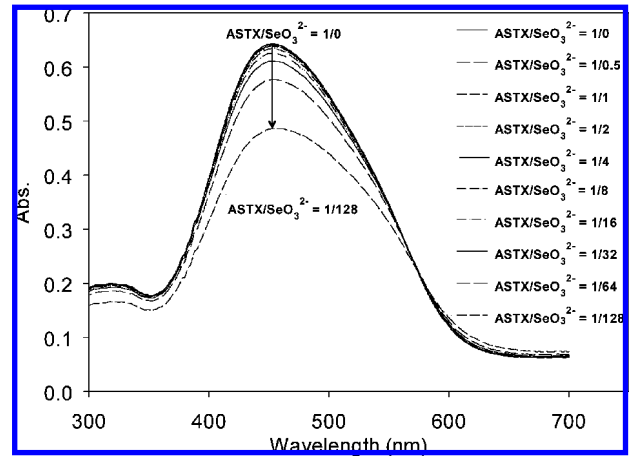

Figure 3. UV/Vis spectra (300−700 nm) of ASTX in DMSO/H_2O (3:17, v/v) titrated with various concentrations of Na_2SeO_3. The maximum absorption was observed at 454 nm. The peak decreased after adding a high concentration of selenite (ASTX/selenite = 1/32).

ppm), a downfield shift (4.32 ppm, Figure 2B) was observed for selenium resonance of ASTX/SeO_3^{2-} (1:1) prepared in mixing DMSO-d_6/D_2O solution. Otherwise, the selenium resonance for SeO_4^{2-} ion was 1050.40 ppm, in which it was indicated that the complexation between ASTX and selenite did not present the redox reaction even though the incubation was more than 12 h. Conversely, as compared to native ASTX, the proton signals of ASTX/SeO_3^{2-} (1:4) were slightly different from the proton signals of native ASTX. The most significant change is that the signals of protons H11 and H15 of ASTX are sharper after incubation with selenite (Figure 2D). Similar to the assumption proposed by Wenk (*42*), this change in the shape of proton signal indicated that the increasing degree of freedom of ASTX was via the entropy-driven process shown in the ITC result.

Changes in Absorption Spectra of ASTX. From the NMR results, the conjugated polyene of ASTX was the binding site for selenite. A similar suggestion was confirmed by monitoring the absorption spectra of ASTX while titrating with Na_2SeO_3 in DMSO/H_2O. The absorbance intensity λ_{max} of ASTX notably decreased within 3 min as the molar ratio of selenite anions increased, as shown in Figure 3. However, the observed decrease in absorbance did not reflect the twist of the chromophore when *trans*-ASTX was isomerized to 9-*cis*-ASTX or 13-*cis*-ASTX in various organic solvents. Incubation of ASTX/SeO_3^{2-} showed an almost identical molar ratio of *trans*-ASTX (from 100 to 95%, data not shown) as with the retention of the all-*trans* configuration of ASTX in DMSO/H_2O within 12 h. The significant decrease of the λ_{max} at 454 nm might have resulted from the alterable conjugation system in the polyene-π-electron influenced by the accretion of Na_2SeO_3. This result is consistent with the lack of an apparent charge transfer band or an obvious shift in absorbance, either red or blue shift.

ASTX Decreases Selenite-Induced Lens Crystallin Turbidity in Vitro. The ability of selenite to cause cataracts in an animal model was first described in 1977 (*16*). However, no report has

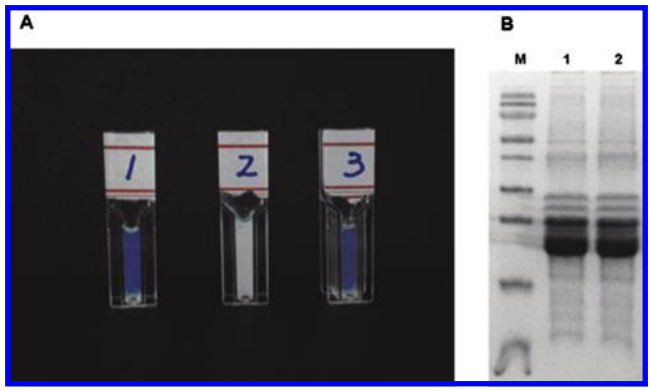

Figure 4. Representative photographs of porcine lens crystallin solutions incubated in three different conditions. (A) Solution 1, porcine lens crystallins; solution 2, porcine lens crystallins with 10 mM sodium selenite; and solution 3, porcine lens crystallins with 10 mM sodium selenate. Porcine lens crystallins became turbid after incubation with selenite for 1 day. The insoluble proteins obtained from turbid samples were then analyzed by SDS-PAGE. (B) Markers (M) with molecular masses from top to bottom were 170, 130, 95, 72, 55, 43, 34, 25, 17, and 11 kDa. Lane 1, porcine crude lens proteins; and lane 2, insoluble proteins obtained from lens proteins incubated with selenite.

indicated how selenite causes the turbidity of lens crystallins. We have incubated lens crystallins with selenite in PBS and found that the crystallin solution became turbid after 1 day of incubation (Figure 4A). The white precipitate was analyzed by SDS-PAGE and indicated that the denatured proteins were similar to that of crude porcine lens proteins (Figure 4B). No obvious degradation of the crystallin was observed, indicating that the precipitate did not result from proteolysis by calpain. We further incubated crystallins with 1 and 10 mM selenite (Na_2SeO_3) or selenate (Na_2SeO_4) in lens buffer, which contained β-mercaptoethanol, to prevent the degradation of crystallins by proteases, especially calpain. As shown in Figure 5A, crystallins incubated with selenite became turbid, while those incubated with selenate remained clear. A report indicated that selenite will react with β-mercaptoethanol, and the generated product, selenodimercaptoethanol, showed minor absorption at wavelengths longer than 400 nm (*43*). Accordingly, we tested this possible interaction by measuring the absorbance of the buffer containing 10 mM selenite at O.D. 450 nm and found it to be negligible. We also added EDTA to the buffer to prevent the degradation of crystallins by metalloproteases. In addition to preventing the degradation, EDTA was added to prevent Ca^{2+}-induced crystallin aggregation.

By using the established assays described above, we then tested the ability of ASTX in preventing selenite-induced lens turbidity. The lens crystallins containing various concentrations (0, 1.25, 2.5, 7.5, and 12.5 μM) of ASTX were then added with 10 mM selenite. The O.D. 450 nm changes (ΔO.D. 450 nm) became smaller with increasing ASTX concentrations, indicating that higher ASTX concentrations attenuated the turbidity formation (Figure 5B). The solvent DMSO by itself produced no effect on turbidity. The ^{77}Se-NMR signal of selenite in DMSO-d_6/D_2O was near 1278.97 ppm, whereas in CH_3CN/$CHCl_3$, it was 1280.02 ppm. No significant change in ^{77}Se-NMR indicated that selenite didn't react with DMSO. ASTX at concentrations of 2.5−12.5 μM significantly inhibited turbidity formation as compared to the control group ($P < 0.05$). Thus, it was shown that ASTX attenuated selenite-induced turbidity in vitro.

ASTX Attenuated in Vivo Selenite-Induced Cataractogenesis. Selenite cataract has been extensively utilized to evaluate

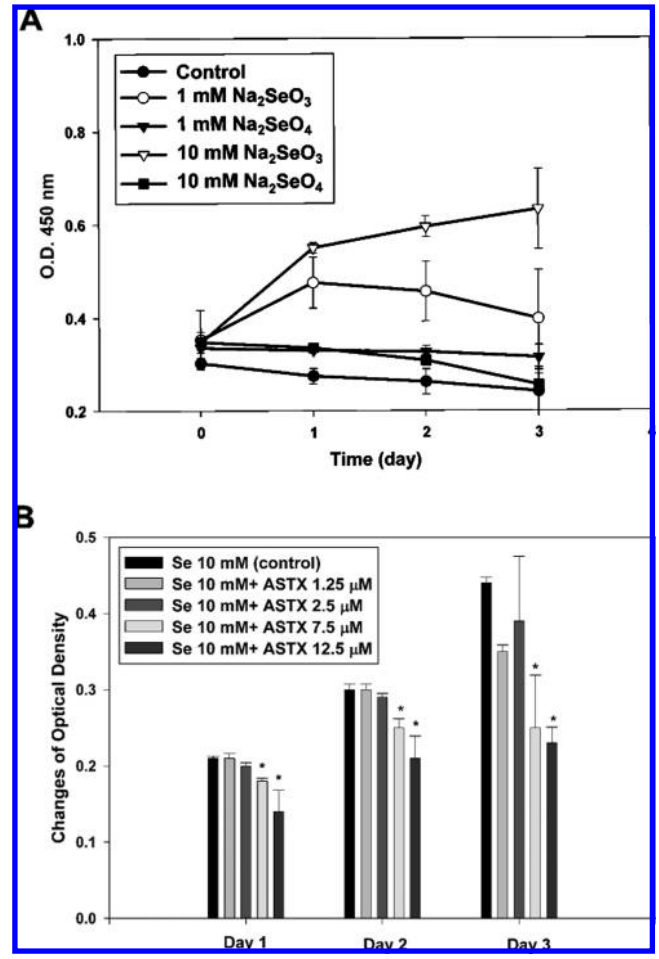

Figure 5. Selenite induces lens turbidity and ASTX attenuates selenite-induced turbidity. (A) The lens crystallins (65 mg/mL) were incubated with 1 and 10 mM selenite (Na_2SeO_3) or selenate (Na_2SeO_4) in buffer containing 50 mM Tris-HCl, 0.1 M NaCl, 5 mM EDTA, 0.01% β-mercaptoethanol, and 0.02% sodium azide, pH 8.0. Crude lens crystallins alone was used as a control. (B) Selenite-induced turbidity of crude lens crystallins was attenuated by ASTX. The lens crystallins (65 mg/mL) were incubated with 10 mM selenite (Na_2SeO_3) in buffer containing 50 mM Tris-HCl, 0.1 M NaCl, 5 mM EDTA, 0.01% β-mercaptoethanol, and 0.02% sodium azide, pH 8.0. The sample containing crude lens crystallins and 10 mM selenite was used as a control. Various concentrations of ASTX were added. The turbidity of each sample was measured at O.D. 450 nm by an ELISA reader daily, and the bars denote ranges of variation from four measurements. *$P <$ 0.05 for comparison with the control group, by One-Way ANOVA with post hoc Dunnett's method.

potential anticataract agents (*44*). These experiments utilized suckling rat pups pretreated with various concentrations of ASTX orally followed by a single subcutaneous injection of high-dose sodium selenite. When the transparency of rat lenses, as shown in Figure 6, was scored and averaged for each treatment group, ASTX at 0.3 and 1 mg/kg decreased the severity of cataract formation. The average score vs each ASTX dosage was calculated and is shown in Figure 6D. There was a statistically significant difference ($p < 0.05$) for the 1.0 mg/kg ASTX-treated group when compared to the control and 0.1 mg/kg ASTX-treated groups.

Discussion

Among the carotenoids, carotene has been reported to protect against cataract formation (*45, 46*). In addition to these epidemiologic studies, lycopene has been reported to attenuate oxidative stress-induced cataract formation (*47*). We have de-

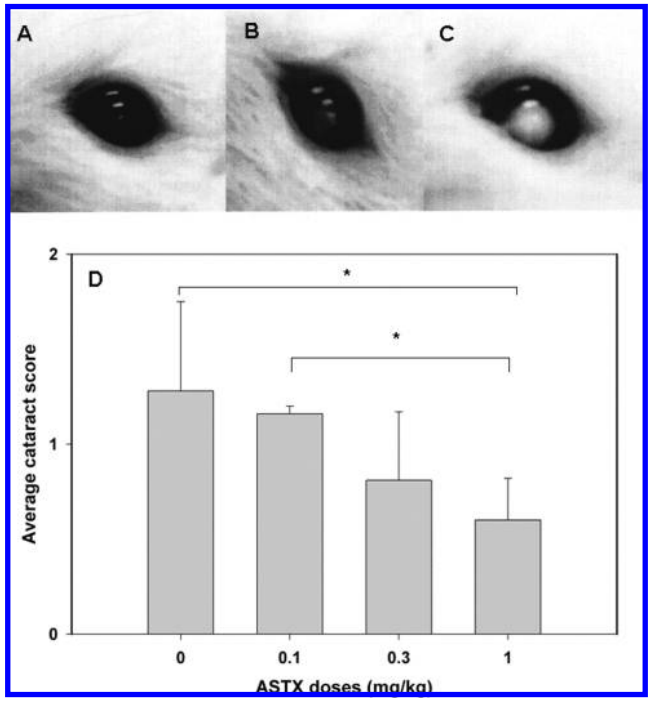

Figure 6. Average cataract scores of groups treated with various doses of ASTX. The selenite-induced cataractogenesis was classified as pinpoint cataract (B) and mature cataract (C) and scored as 1 and 2, respectively, while the normal lens was scored as 0 (A). The average lens cataract score for each group ($n = 10-18$) following oral administration (0, 0.1, 0.3, and 1 mg/kg) of ASTX is expressed as a mean ± standard error and is plotted as shown in panel D. The average cataract scores decreased from 1.3 ± 0.4 to 0.5 ± 0.2 with increasing treatment doses of ASTX. The asterisk indicates that the average cataract score of the 1 mg/kg ASTX-treated group was significantly different from the ones of the control (0 mg/kg) and 0.1 mg/kg ASTX-treated groups ($p < 0.05$).

monstrated the in vitro ability of ASTX to protect porcine lens crystallins against oxidative damage by iron-mediated hydroxyl radicals or proteolysis by calcium ion-activated calpain (*38*). Such activity is further supported by the in vitro properties of the ASTX/Ca^{2+} complex (*39*). However, there are no reports describing the possible involvement of a selenite-quenching mechanism for these observed anticataract agents, especially via a direct interaction with selenite.

Our current results from ITC demonstrated that ASTX interacted with selenite but not with selenate (Figure 1). According to the ^{1}H NMR spectrum of ASTX/selenite, there was no newly-formed signals, which indicated that a chemical reaction between selenite and ASTX did not occur. The ^{77}Se-NMR signals of selenite and selenate were at 1278.97 and 1050.40 ppm, respectively, and indicated that ASTX interacted with selenite with a 4.32 ppm downfield shift (Figure 2) in the selenium NMR spectrum. These findings support the results obtained with ITC. On the other hand, that the ^{77}Se-NMR signal of selenite/ASTX was very near the signal of selenite indicated that there was no significant change in the oxidative state of selenium. These data point to ASTX as having a selective binding affinity with the selenite ion. Comparison of the ^{1}H NMR spectrum of ASTX/selenite with that of ASTX alone showed a very slight change in the signals for the conjugated polyenes, especially protons H11 and H15 of ASTX (Figure 2). Because selenite interacts with conjugated polyenes, the absorption spectra of ASTX when titrated with Na_2SeO_3 would be expected to reflect such an observation. The decreasing magnitude of the absorption peak with the increased selenite concentrations indicates that the conjugated system of ASTX interacted with selenite (Figure 3). The single peak absorption of ASTX at 454 nm presents the feature of H-type aggregates of ASTX (*48*). There was no involvement of positively charged polyenes formation since no maximum absorption shift occurred (*35*). The involvement of the chromophore changes due to *cis*−*trans* isomerizations was also excluded since HPLC analysis showed an almost identical molar ratio of *cis*-ASTX:*trans*-ASTX in ASTX/SeO_3^{2-} or ASTX (see the Supporting Information). The FT-IR studies of ASTX/SeO_3^{2-} and ASTX solutions indicated that there was no change in the carbonyl group of ASTX (see the Supporting Information). Retracing the ^{1}H NMR spectra of ASTX/SeO_3^{2-} and ASTX, no significant changes were observed in the hydroxyl groups of ASTX. Taken together, the interaction between ASTX and selenite was at the conjugated polyene of ASTX. ASTX with an electron-rich π-conjugated moiety interacting coordinately with electron-poor selenium of SeO_3^{2-} would result in a shielding effect and further reflected to the downfield shift of the NMR spectra. The results were consistent with an earlier study showing that selenium binds to the lipids of marine algae (*41*). In that study, selenium was thought to be bound to the lipids, such as carotenoid pigments, rather than metabolically incorporated. It was presumed that selenium binded to double bonds in the lipids. Pigments that contain most of the double bonds were found to contain most of the selenium when extracted. Lipids without double bonds or with disruption of double bonds lacked selenium in the extracts. Such an interaction manner is different from the one interacting with proteins through hydrophobic interaction occurring in marine animals (*49*).

Because there was no bond formation between ASTX and selenite, the energy change in the ITC experiment could be viewed as the result of binding. From the one-site fitting function with stoichiometry $n = 2.12$, the interaction between ASTX and selenite was observed with an enthalpy-capture process, a large entropy property, and a negative Gibb's free energy ($\Delta H = 7.65$ kcal/mol, $\Delta S = 42.4$ cal mol^{-1} K^{-1}, and $\Delta G = -4.99$ kcal/mol). Although we could not identify the heats of association and dissociation individually, the stoichiometry between ASTX and selenite is estimated to be 2. The large entropy property implied that the degree of freedom increased during complexation formation of ASTX/SeO_3^{2-}. However, the complexation of two molecules should have allowed the degree of freedom to decrease. It has been reported that ASTX forms self-assembly in an acetone/water solution (*48*). Our results of the UV/vis spectra indicated that ASTX forms face-to-face H-type self-assembly in a DMSO/water solution (Figure 3). From this point of view, the stoichiometry $n = 2.12$ could be explained and responded to a ASTX/SeO_3^{2-} = 3/6 self-assembly supramolecule reasonably, and the polyene group of ASTX could provide the binding ability with SeO_3^{2-} from the axial positions of the triangular face of the selenite ion. In a solvated or hydrated selenite ion, the formation of ASTX/SeO_3^{2-} supramolecule would isolate six selenite ions and release the 12 solvent molecules; as a result, an increase in the entropy during the supramolecule formation is observed in the ITC experiment. The insertion of selenite ions into the H-type self-assembly ASTX could be combined with multiple steps, including decreasing the hydrophobic interaction between the ASTX, increasing the formation of the ASTX/SeO_3^{2-} complexation, and decreasing the solvating network of selenite ions (see the Supporting Information, Figure S17). Endothermal enthalpy from decreasing processes could not be compensated from the exothermal enthalpy process, and a positive enthalpy is observed in the ITC experiment. Added to this, the ITC titration is

performed from a 0 to 4.5 molar ratio of SeO_3^{2-}/ASTX, and the presented model can only be applied to explain the SeO_3^{2-}/ASTX interaction during the selenite insertion into the H-type ASTX. From the UV/Vis titration experiment (Figure 3), the absorption obviously drops after the ratio ASTX/SeO_3^{2-} = 1/32. Formation of the ASTX/SeO_3^{2-} complex might lead to the dissociation of ASTX self-assembly with a higher molar ratio of selenite ions. The presented data in hand could not support the hypothesis of the dissociation; however, the interaction between the ASTX and the selenite is supported and proved.

Several biochemical processes occur during selenite-induced cataract formation, and both calcium accumulation and calpain-induced proteolysis are key steps (*13*). The in vitro calcium-induced porcine lens turbidity assay has been established in our laboratory as a model of cataractogenesis (*38*). Here, we incubated lens crystallin with selenite ions and found that the crystallin solution became turbid after only 1 day of incubation at 37 °C (Figure 4A). SDS-PAGE analysis revealed that the turbidity of the crystallins was due to the precipitation of lens protein and not related to calpain (Figure 4B). Because it was reported that calcium-induced lens turbidity could be inhibited by ASTX in our previous study, to rule out any calcium-related protective mechanism, a buffer containing β-mercaptoethanol and EDTA capable of minimizing the crystallin proteolysis was chosen to replace the phosphate buffer used in Figure 4A, and similar results were observed (Figure 5A). Those results not only confirm the earlier reported selenite-induced sulfhydryl oxidation of lens proteins (*50*) but also unambiguously clarify the formation of α-crystallin aggregates (*51*). The results of previous experiments that ^{75}Se accumulated in the soluble and insoluble proteins of the lens (*52*) and cortical opacities developed in a selenite-containing medium (*47*) provide evidence that selenite enters the lens. Our results allow us to propose that accumulation of selenite in lens may cause cataract formation directly and provide a rational explanation for the high selenium content present with increasing opacification in human lenses (*9*). It should be noted that cataracts constitute a multifactorial disease process associated with many risk factors. Oxidation of critical sulfhydryl groups of Ca^{2+}-ATPase on lens epithelial membrane by selenite, influx and accumulation of calcium ions (*19*), and cleavage of N-terminal extension of β-crystallins by calpain all are associated with selenite cataractogenesis (*53*). As well as the above factors, accumulation of selenite in the lens can be another risk factor of selenite-induced cataracts. Because selenite is capable of inducing the turbidity of porcine lens crystallins, similar reactions may occur between selenite and the rat lens crystallins because vertebrates have similar amino acid sequences of crystallins (*54, 55*).

The in vitro test of selenite-induced crystallin turbidity demonstrated that the changes of O.D. 450 nm (ΔO.D. 450 nm) were decreased with increasing ASTX concentration (Figure 5B). That decreases in ΔO.D. 450 nm occurred indicates that ASTX is capable of attenuating selenite-induced crystallin turbidity. The direct interactions of ASTX and selenite may be responsible for the minimization of selenite-induced turbidity of lenticular crystallins. The initial slight decreases in O.D. value of the crystallin solution containing ASTX after the addition of selenite were also consistent with our spectroscopic results. Previous studies have revealed that the thiol group would likely react with selenite (*56*). Therefore, it was presumed that selenite may interact with thiol groups of crystallins and lead to precipitation of crystallins, while ASTX may tend to trap selenite away from the thiol groups. According to our ITC results, even though the fitting association constant approximated 4.6×10^3,

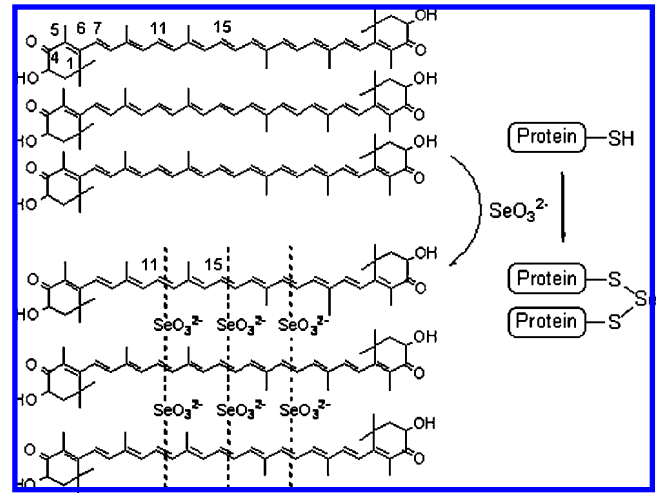

Figure 7. Hypothesis for ASTX in attenuating selentie-induced cataractogenesis. It was proposed that ASTX may tend to trap selenite away from the thiol groups to minimize the precipitation of crystallins when selenite interacts with thiol groups of crystallins.

which indicated that ASTX interacted with selenite weakly, thiol groups interact with selenite by bonding with the selenium atom and must overcome the activation energy. Therefore, selenite ions would likely interact with ASTX first, rather than with the thiol group, and would result in amelioration of selenite-induced crystallin turbidity by ASTX (Figure 7).

On the basis of the above findings of the in vitro studies, ASTX was then evaluated in vivo in a cataract animal model by subcutaneously administering a high dose of selenite. The percentage of rats with extremely clear lenses increased with increasing oral dose of ASTX, while the percentage of rats with mature dense opacity lenses was decreased with increasing doses of ASTX. It is clear that ASTX attenuates selenite-induced cataractogenesis in rat in a dose-dependent manner (Figure 6D). Similarly, it also has been reported that lycopene attenuates selenite-induced cataracts (*47*). The levels of superoxide dismutase, catalase, and glutathione S-transferase were elevated in the presence of lycopene, indicating that lycopene's ability to attenuate selenite-induced cataract is related to the antioxidant defense of the lens. However, some doubt remains regarding the mechanisms of improving antioxidant defenses of the lens. Because ASTX and lycopene are members of the carotenoid family, ASTX may have some similar effects to lycopene. In animal models, the situation is much more complex than in vitro tests, and we could not exclude this possibility of improving the antioxidant defense mechanism of the lens. Several biochemical processes involved in the formation of selenite-induced cataracts, for example, selenite-induced metabolism alternation in the lens epithelium, and the toxicity of selenite through hydrogen selenide have been reported recently (*57*). In addition, glutathione and selenite may spontaneously react to produce hydrogen selenide and reactive oxygen species, which may further damage the lens epithelium. However, maintenance of regular endogenous glutathione levels by antioxidants could prevent selenite from interacting with crystallins. The potential involvement of the interactions between ASTX and selenite in preventing the reactions of glutathione and selenite require further investigations.

In conclusion, our results allow us to propose that accumulation of selenite in the lens may cause cataract formation directly. This is the first report of a direct interaction of ASTX with selenite by ITC and a delayed selenite-induced lens crystallin precipitation by ASTX. The interaction of ASTX with selenite

is through conjugated polyene, and this convenient assay system for anticataract agents via a selenite-quenching mechanism provides us a new aspect in cataractogenesis.

Acknowledgment. We greatly appreciate Dr. Shu-Chuan Jao for her technical support regarding NMR spectra and the isothermal titration calorimeter. This study was supported by grants from the National Science Council (Taipei, Taiwan).

Supporting Information Available: Titration experiments of ASTX with Na_2SeO_4, Na_2SO_3, and Na_2SO_3 measured with ITC, UV/Vis, and NMR methods. HPLC profile and FT-IR spectra for ASTX/Na_2SeO_3 and ASTX/Na_2SeO_4 mixtures. This material is available free of charge via the Internet at http://pubs.acs.org.

References

(1) Mugesh, G., du Mont, W. W., and Sies, H. (2001) Chemistry of biologically important synthetic organoselenium compounds. *Chem. Rev. 101*, 2125–2179.
(2) Bergomi, M., Vinceti, M., Nacci, G., Pietrini, V., Bratter, P., Alber, D., Ferrari, A., Vescovi, L., Guidetti, D., Sola, P., Malagu, S., Aramini, C., and Vivoli, G. (2002) Environmental exposure to trace elements and risk of amyotrophic lateral sclerosis: a population-based case-control study. *Environ. Res. 89*, 116–123.
(3) Cooper, L. T., Rader, V., and Ralston, N. V. (2007) The roles of selenium and mercury in the pathogenesis of viral cardiomyopathy. *Congestive Heart Failure 13*, 193–199.
(4) Navarro Silvera, S. A., and Rohan, T. E. (2007) Trace elements and cancer risk: A review of the epidemiologic evidence. *Cancer Causes Control 18*, 7–27.
(5) Alexander, J. (2007) Selenium. *Novartis Found Symp. 282*, 143.
(6) Levander, O. A., and Mertz, W., Eds. (1986) *Trace Elements in Human and Animal Nutrition*, 209 pp, Academic Press Orlando, Florida.
(7) Spiller, H. A., and Pfiefer, E. (2007) Two fatal cases of selenium toxicity. *Forensic Sci. Int. 171*, 67–72.
(8) Karakucuk, S., Ertugrul Mirza, G., Faruk Ekinciler, O., Saraymen, R., Karakucuk, I., and Ustdal, M. (1995) Selenium concentrations in serum, lens and aqueous humour of patients with senile cataract. *Acta Ophthalmol. Scand. 73*, 329–332.
(9) Dawczynski, J., Winnefeld, K., Konigsdorffer, E., Augsten, R., Blum, M., and Strobel, J. (2006) Selenium and cataract—Risk factor or useful dietary supplement? *Klin. Monatsbl. Augenheilkd. 223*, 675–680.
(10) Klayman, D. L., and Günther, W. H. H. G., Eds. (1973) *Organic Selenium Compounds: Their Chemistry and Biology*, John Wiley & Sons, Inc., New York.
(11) Barceloux, D. G. (1999) Selenium. *J. Toxicol. Clin. Toxicol. 37*, 145–172.
(12) Schrauzer, G. N. (2001) Nutritional selenium supplements: Product types, quality, and safety. *J. Am. Coll. Nutr. 20*, 1–4.
(13) Shearer, T. R., Ma, H., Fukiage, C., and Azuma, M. (1997) Selenite nuclear cataract: Review of the model. *Mol. Vis. 3*, 8.
(14) Babicky, A., Rychter, Z., Kopoldova, J., and Ostadalova, I. (1985) Age dependence of selenite uptake in rat eye lenses. *Exp. Eye Res. 40*, 101–103.
(15) Ostadalova, I., and Babicky, A. (1980) Toxic effect of various selenium compounds on the rat in the early postnatal period. *Arch. Toxicol. 45*, 207–211.
(16) Ostadalova, I., Babicky, A., and Obenberger, J. (1978) Cataract induced by administration of a single dose of sodium selenite to suckling rats. *Experientia 34*, 222–223.
(17) Ostadalova, I., Babicky, A., and Obenberger, J. (1979) Cataractogenic and lethal effect of selenite in rats during postnatal ontogenesis. *Physiol. Bohemoslov. 28*, 393–397.
(18) Hightower, K. R., and McCready, J. P. (1991) Effect of selenite on epithelium of cultured rabbit lens. *Invest. Ophthalmol. Vis. Sci. 32*, 406–409.
(19) Wang, Z., Bunce, G. E., and Hess, J. L. (1993) Selenite and Ca^{2+} homeostasis in the rat lens: Effect on Ca-ATPase and passive Ca^{2+} transport. *Curr. Eye Res. 12*, 213–218.
(20) Orhan, H., Marol, S., Hepsen, I. F., and Sahin, G. (1999) Effects of some probable antioxidants on selenite-induced cataract formation and oxidative stress-related parameters in rats. *Toxicology 139*, 219–232.
(21) Guerin, M., Huntley, M. E., and Olaizola, M. (2003) Haematococcus astaxanthin: Applications for human health and nutrition. *Trends Biotechnol. 21*, 210–216.
(22) Naguib, Y. M. (2000) Antioxidant activities of astaxanthin and related carotenoids. *J. Agric. Food Chem. 48*, 1150–1154.
(23) Palozza, P., and Krinsky, N. I. (1992) Astaxanthin and canthaxanthin are potent antioxidants in a membrane model. *Arch. Biochem. Biophys. 297*, 291–295.
(24) Terao, J. (1989) Antioxidant activity of beta-carotene-related carotenoids in solution. *Lipids 24*, 659–661.
(25) Kang, J. O., Kim, S. J., and Kim, H. (2001) Effect of astaxanthin on the hepatotoxicity, lipid peroxidation and antioxidative enzymes in the liver of CCl4-treated rats. *Methods Find Exp. Clin. Pharmacol. 23*, 79–84.
(26) Jyonouchi, H., Sun, S., Iijima, K., and Gross, M. D. (2000) Antitumor activity of astaxanthin and its mode of action. *Nutr. Cancer 36*, 59–65.
(27) Bennedsen, M., Wang, X., Willen, R., Wadstrom, T., and Andersen, L. P. (1999) Treatment of H. pylori infected mice with antioxidant astaxanthin reduces gastric inflammation, bacterial load and modulates cytokine release by splenocytes. *Immunol. Lett. 70*, 185–189.
(28) Wang, X., Willen, R., and Wadstrom, T. (2000) Astaxanthin-rich algal meal and vitamin C inhibit *Helicobacter pylori* infection in BALB/cA mice. *Antimicrob. Agents Chemother. 44*, 2452–2457.
(29) Ohgami, K., Shiratori, K., Kotake, S., Nishida, T., Mizuki, N., Yazawa, K., and Ohno, S. (2003) Effects of astaxanthin on lipopolysaccharide-induced inflammation in vitro and in vivo. *Invest. Ophthalmol. Vis. Sci. 44*, 2694–2701.
(30) Waagbo, R., Hamre, K., Bjerkas, E., Berge, R., Wathne, E., Lie, O., and Torstensen, B. (2003) Cataract formation in Atlantic salmon, *Salmo salar* L., smolt relative to dietary pro- and antioxidants and lipid level. *J. Fish Dis. 26*, 213–229.
(31) Buchwald, M., and Jencks, W. P. (1968) Optical properties of astaxanthin solutions and aggregates. *Biochemistry 7*, 834–843.
(32) Salares, V. R., Young, N. M., Bernstein, H. J., and Carey, P. R. (1979) Mechanisms of spectral shifts in lobster carotenoproteins. The resonance Raman spectra of ovoverdin and the crustacyanins. *Biochim. Biophys. Acta 576*, 176–191.
(33) Weesie, R. J., Jansen, F. J., Merlin, J. C., Lugtenburg, J., Britton, G., and de Groot, H. J. (1997) ^{13}C Magic angle spinning NMR analysis and quantum chemical modeling of the bathochromic shift of astaxanthin in alpha-crustacyanin, the blue carotenoprotein complex in the carapace of the lobster *Homarus gammarus*. *Biochemistry 36*, 7288–7296.
(34) Bartalucci, G., Coppin, J., Fisher, S., Hall, G., Helliwell, J. R., Helliwell, M., and Liaaen-Jensen, S. (2007) Unravelling the chemical basis of the bathochromic shift in the lobster carapace; new crystal structures of unbound astaxanthin, canthaxanthin and zeaxanthin. *Acta Crystallogr. B 63*, 328–337.
(35) Kildahl-Andersen, G., Anthonsen, T., and Liaaen-Jensen, S. (2007) Longer polyenyl cations in relation to soliton theory. *Org. Biomol. Chem. 5*, 2803–2811.
(36) Lutnaes, B. F., Kildahl-Andersen, G., Krane, J., and Liaaen-Jensen, S. (2004) Delocalized carotenoid cations in relation to the soliton model. *J. Am. Chem. Soc. 126*, 8981–8990.
(37) Kildahl-Andersen, G., Lutnaes, B. F., Krane, J., and Liaaen-Jensen, S. (2003) Structure elucidation of polyene systems with extensive charge delocalization-carbocations from allylic carotenols. *Org. Lett. 5*, 2675–2678.
(38) Wu, T. H., Liao, J. H., Hou, W. C., Huang, F. Y., Maher, T. J., and Hu, C. C. (2006) Astaxanthin protects against oxidative stress and calcium-induced porcine lens protein degradation. *J. Agric. Food Chem. 54*, 2418–2423.
(39) Chen, C. S., Wu, S. H., Wu, Y. Y., Fang, J. M., and Wu, T. H. (2007) Properties of astaxanthin/Ca^{2+} complex formation in the deceleration of cis/trans isomerization. *Org. Lett. 9*, 2985–2988.
(40) Laemmli, U. K. (1970) Cleavage of structural proteins during the assembly of the head of bacteriophage T4. *Nature 227*, 680–685.
(41) Gennity, J. M., Bottino, N. R., Zingaro, R. A., Wheeler, A. E., and Irgolic, K. J. (1984) The binding of selenium to the lipids of two unicellular marine algae. *Biochem. Biophys. Res. Commun. 118*, 176–182.
(42) Wenk, M. R., Alt, T., Seelig, A., and Seelig, J. (1997) Octyl-beta-D-glucopyranoside partitioning into lipid bilayers: Thermodynamics of binding and structural changes of the bilayer. *Biophys. J. 72*, 1719–1731.
(43) Ganther, H. E. (1968) Selenotrisulfides. Formation by the reaction of thiols with selenious acid. *Biochemistry 7*, 2898–2905.
(44) Hiraoka, T., Clark, J. I., Li, X. Y., and Thurston, G. M. (1996) Effect of selected anti-cataract agents on opacification in the selenite cataract model. *Exp. Eye Res. 62*, 11–19.
(45) Gale, C. R., Hall, N. F., Phillips, D. I., and Martyn, C. N. (2001) Plasma antioxidant vitamins and carotenoids and age-related cataract. *Ophthalmology 108*, 1992–1998.
(46) Brown, L., Rimm, E. B., Seddon, J. M., Giovannucci, E. L., Chasan-Taber, L., Spiegelman, D., Willett, W. C., and Hankinson, S. E. (1999) A prospective study of carotenoid intake and risk of cataract extraction in US men. *Am. J. Clin. Nutr. 70*, 517–524.

(47) Gupta, S. K., Trivedi, D., Srivastava, S., Joshi, S., Halder, N., and Verma, S. D. (2003) Lycopene attenuates oxidative stress induced experimental cataract development: An in vitro and in vivo study. *Nutrition 19*, 794–799.
(48) Kopsel, C., Moltgen, H., Schuch, H., Auweter, H., Kleinermanns, K., Martin, H., and Bettermann, H. (2005) Structure investigations on assembled astaxanthin molecules. *J. Mol. Struct. 750*, 109–115.
(49) Cianci, M., Rizkallah, P. J., Olczak, A., Raftery, J., Chayen, N. E., Zagalsky, P. F., and Helliwell, J. R. (2002) The molecular basis of the coloration mechanism in lobster shell: Beta-crustacyanin at 3.2-A resolution. *Proc. Natl. Acad. Sci. U.S.A. 99*, 9795–9800.
(50) Guo, S. B., Manabe, S., and Wada, O. (1989) The decomposition and aggregation of rat lens protein induced by selenite in vitro and in vivo. *Nippon Eiseigaku Zasshi 44*, 615–621.
(51) Yan, H., Harding, J. J., Hui, Y. N., and Li, M. Y. (2003) Decreased chaperone activity of alpha-crystallin in selenite cataract may result from selenite-induced aggregation. *Eye 17*, 637–645.
(52) Shearer, T. R., Anderson, R. S., and Britton, J. L. (1982) Uptake and distribution of radioactive selenium in cataractous rat lens. *Curr. Eye Res. 2*, 561–564.
(53) David, L. L., Shearer, T. R., and Shih, M. (1993) Sequence analysis of lens beta-crystallins suggests involvement of calpain in cataract formation. *J. Biol. Chem. 268*, 1937–1940.
(54) de Jong, W. W., Caspers, G. J., and Leunissen, J. A. (1998) Genealogy of the alpha-crystallin—Small heat-shock protein superfamily. *Int. J. Biol. Macromol. 22*, 151–162.
(55) Bloemendal, H., and de Jong, W. W. (1991) Lens proteins and their genes. *Prog. Nucleic Acid Res. Mol. Biol. 41*, 259–281.
(56) Painter, E. (1941) The chemistry and toxicity of selenium compounds, with special reference to the selenium problem. *Chem. Rev. 28*, 179–213.
(57) Tarze, A., Dauplais, M., Grigoras, I., Lazard, M., Ha-Duong, N. T., Barbier, F., Blanquet, S., and Plateau, P. (2007) Extracellular production of hydrogen selenide accounts for thiol-assisted toxicity of selenite against *Saccharomyces cerevisiae*. *J. Biol. Chem. 282*, 8759–8767.

TX800378Z